Experimental Study of Channel Estimation Algorithms for General IRS Applications

Yueheng Li*[1], Sven Bettinga, Frieder Gedenk, Xueyun Long*, Mohammad Basim Alabd*, Lucas Giroto de Oliveira*, and Thomas Zwick*

*Institute of Radio Frequency Engineering and Electronics (IHE),
Karlsruhe Institute of Technology (KIT), 76131, Karlsruhe, Germany
[1]yueheng.li@kit.edu

***Abstract* — An intelligent reflecting surface (IRS) is a promising antenna array concept capable of realizing flexible electronically steerable beamforming. Depending on the location of the feeding antenna, IRS applications can be classified as either nearfield or farfield types. Using the IRS operating at $28\,\mathrm{GHz}$, both application types are analyzed and compared in this paper. On the IRS testbed, channel estimation algorithms, including beam training and IRS unit channel state information (CSI) estimation, are implemented and analyzed for both application types. The results of the measurements indicate that the aforementioned algorithms are adaptable to both IRS application types. In addition, the IRS coding patterns designed using the estimated CSI at each IRS unit outperform the pre-designed patterns for beam training when constructing the wireless communication link. This paper provides evidence that IRS-based theoretical algorithms can be implemented in practice.**

***Keywords* — digital signal processing, communication systems, antenna arrays, intelligent reflecting surface**

I. Introduction

With the evolution of wireless communication technologies, beamforming has become a prevalent method for overcoming the increasing free space path loss for wideband signal propagation at higher carrier frequencies. An antenna array with controllable phase shifts at the antenna units directs power to the desired areas to achieve beamforming. An intelligent reflecting surface (IRS), also known as a programmable metasurface, a reconfigurable intelligent surface, is one of the available solutions [1]. Massive micro-component-based antenna units construct the IRS using conventional solutions such as PIN diodes or varactors. By illuminating the IRS with a feeding antenna, electronically controllable beamforming is realized with appropriate costs and power consumption, which may offer future concepts and marketing advantages. In recent years, fruitful IRS designs have popped up, with representative products in [1], [2].

The IRS is primarily studied for two application types at the current research stage. According to [3], these application types can be differentiated based on the spatial position of the feeding antenna. The feeding antenna for the first type is located in the nearfield of IRS. In this case, the IRS is considered an alternative antenna array. [4] has presented proofs of concept for the combination of digital signal processing and IRS wireless communication. IRSs are also integrated with advanced wireless communication technologies, such as time division multiple access [5], mobile tracking [6], and hybrid beamforming [7]. The feeding antenna for the second type is located in the farfield of IRS. As stated in [8], the IRS is regarded as a signal reflector that offers solid reflectional access between the transmitter and receiver. This novel concept obtains significant scientific interest. For instance, channel estimation algorithms have been examined in [9]. The IRSs are integrated with the multiple-input multiple-output (MIMO) system described in [10] for multiuser scenarios. Techniques integrating hybrid beamforming and hierarchical codebook channel estimation have been developed in [11]. For system demonstration, [12] provides measurements for propagation distances up to $500\,\mathrm{m}$ at $5.8\,\mathrm{GHz}$.

In general, the two aforementioned application types share the same IRS design specification, which leads to joint research [3]. However, experimental studies in combination with signal processing algorithms are missing. The relationships between nearfield and farfield applications are first investigated in this paper. Based on the outcomes, the beam training channel estimation algorithm for nearfield application in [7] is adapted for farfield application. Next, the theoretical channel estimation algorithm based on Hadamard-matrix truncation from [13] supports a novel system-level implementation for both application types. For the sake of completeness, the aforementioned channel estimation algorithms are compared with measurement results.

II. IRS Application Types

In this section, the general definition for nearfield and farfield IRS application types will be introduced and compared, as a review of their conventional definitions.

A. IRS Nearfield Application

In Figure 1a, a general model for IRS nearfield application is depicted. With the feeding antenna in the nearfield of IRS, the entire system is considered an alternative antenna array, such as the one used at a base station (BS). For nearfield illumination, the feeding antenna behaves as a point source to the IRS, with each antenna unit having a unique incidence angle, illuminated power, and illumination distance. These effects result in illumination loss and spillover

loss, which necessitate an optimization of the antenna's geometrical setup in order to achieve maximum gain [14]. For the wireless channel, a single-input single-output (SISO) architecture including IRS beamforming can be expressed as

$$s_{Rx} = \boldsymbol{h}_n \boldsymbol{f} s_{Tx} + w. \quad (1)$$

IRS is assumed to be equipped only at Tx for the sake of simplicity, and no additional signal processing is applied in this paper. The terms s_{Rx} and s_{Tx} are received signal and transmit symbol, respectively, assuming a single time interval or frequency slot. The vector $\boldsymbol{h}_n \in \mathbb{C}^{1\times MN}$ represents the channel between each IRS unit to the receive antenna, with M and N denoting the total number of IRS elements along the 2-dimensional (2D) plane. The term w denotes the noise contribution. The vector $\boldsymbol{f} \in \mathbb{C}^{MN\times 1}$ represents the IRS beamforming containing unit cell phase shifts. In contrast to a phased array with variable gain amplifiers integrated into the circuits, IRS beamforming is achieved by controlling the illuminated electromagnetic wave using antenna units comprised of microcomponents. In such designs, the amplitudes of each unit cell are regarded as fixed, untunable quantities. Therefore, the most important task is to accurately compute the phase distribution at each antenna unit.

B. IRS Farfield Application

Fig. 1b depicts a general model for the farfield application of the IRS. With the feeding antenna in the farfield of IRS, IRS serves as a signal reflector to create a reflection path from the transmitter BS to the receiver user equipment (UE). For farfield illumination, the IRS considers the feeding antenna to be a source of plane waves. Consequently, the incidence angle, illuminated power, and illumination distance are distributed uniformly across all antenna units. Considering the channel model, the IRS splits the entire wireless channel into two parts, namely incidence channel $\boldsymbol{h}_1 \in \mathbb{C}^{MN\times 1}$ and reflection channel $\boldsymbol{h}_2 \in \mathbb{C}^{1\times MN}$. Therefore, assuming a SISO architecture, the received symbol becomes

$$s_{Rx} = \boldsymbol{h}_2 \boldsymbol{F} \boldsymbol{h}_1 s_{Tx} + w. \quad (2)$$

The beamforming from IRS is represented by the diagonal matrix $\boldsymbol{F} \in \mathbb{C}^{MN\times MN}$. Each diagonal element contains the phase shift contribution of the corresponding IRS unit.

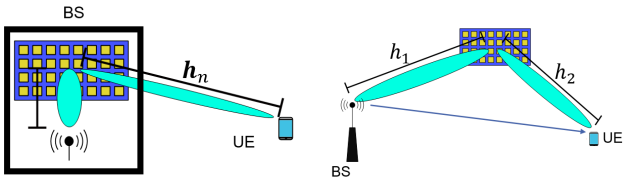

(a) IRS as antenna array. (b) IRS as signal reflector.

Fig. 1. IRS application types.

III. IRS Channel Estimation

Based on (1) and (2), it can be observed that the determination of phase shifts at the IRS unit cells dominates the received signal quality, yielding the IRS coding pattern. In this section, different algorithms to determine the IRS coding pattern will be introduced.

A. IRS Beam Training

Beam training is an algorithm to search for the direction of departure (DoD) or direction of arrival (DoA) between the transmitter and receiver using pre-designed beamforming patterns [15]. After the DoD/DoA is determined, a simple least-square (LS) method can be implemented to derive the detailed channel coefficient for the assumed SISO case. To operate beam training, it is critical to ensure a proper beamforming pattern at the antenna array, which corresponds to the IRS coding pattern. According to [3] and [6], one of the general solutions to realize beamforming at the IRS is to individually control the phase at each unit following

$$\varphi(m,n,\theta,\phi) = e^{-j\kappa\cdot(md\sin\theta\cos\phi + nd\sin\theta\sin\phi)+\varphi_d(m,n)}. \quad (3)$$

Here, m and n are the unit indexes for the 2D IRS. The variables θ, ϕ indicate the beamforming direction, with θ to be the tilt angle perpendicular to the IRS plane, and ϕ to be the rotation angle in the IRS plane. The term $\kappa = \frac{2\pi}{\lambda}$ is the wave constant. The variable d is the antenna spacing between each unit, with a uniform planar array assumed in this paper. The special factor in (3) is the additive phase $\varphi_d(m,n)$. This term compensates for the additional phase shifts at each IRS unit introduced by the varying distance between different IRS units and the feeding antenna phase center.

In previous studies, beam training was primarily utilized for channel estimation in nearfield IRS applications, due to the difficulties for channel state information (CSI) derivation at each IRS unit [7]. This can be realized by correctly adjusting the phase vector $\boldsymbol{f}$ from (1) based on (3). With a pre-defined beam training range and resolution, pre-computed IRS coding patterns are examined according to a quality index, e.g., receiver power. Afterwards, the DoD/DoA is determined by the beamforming direction that offers the best quality index performance.

Since the key feature for beam training is the beamforming pattern at the IRS, it is also expected to work for farfield application if the phase distribution matrix $\boldsymbol{F}$ in (2) is properly adjusted. In most cases, BS and IRS are stationary components in the wireless communication link. Therefore, beam training is only required for the path from the IRS to the UE. Following (3), the farfield beamforming can be generated with the additive phase $\varphi_d(m,n)$ vanishes due to the plane wave illumination characterization mentioned in Section II-B. In this case, the part $\boldsymbol{F}\boldsymbol{h}_1$ from (2) is reformulated to a beam steering vector which approaches the $\boldsymbol{f}$ in (1). Possible differences happen at the received signal regarding the magnitude, phase and delay profile due to the reflectional path, but they can be simply derived with the least square (LS) method by computing the ratio between the received and transmit symbols.

B. IRS Unit CSI

With the development of research, more theoretical solutions for IRS channel estimation are created with sufficient practical considerations for experimental studies. In practical IRS scenarios, there are additional contributions caused by any path independent of IRS from the transmitter to the receiver. Especially for the farfield IRS application in Fig.

1b, there can be a strong LoS path from the transmitter to the receiver. If these contributions can be considered in the channel estimation, better system performance is available. An equivalent SISO IRS channel of (2) based on [13] is expressed as

$$h = \boldsymbol{h_e}\boldsymbol{\varphi} + h_c. \tag{4}$$

The vector $\boldsymbol{\varphi} = [\varphi_1, ..., \varphi_{MN}]^T$ denotes the IRS unit phase shifts. The vector $\boldsymbol{h_e} = \boldsymbol{h}_2 \text{diag}(\boldsymbol{h}_1)$ represents a cascaded IRS reflection channel. The additional term h_c represents the IRS independent contribution. The expression from (4) can be further simplified as $h = \boldsymbol{h_f}\boldsymbol{\varphi_f}$, with $\boldsymbol{h_f} = [h_c, \boldsymbol{h_e}]$, and $\boldsymbol{\varphi_f} = [1, \boldsymbol{\varphi}]$. It can be observed that even though the channel model is transformed from the farfield application, the effective channel $h = \boldsymbol{h_f}\boldsymbol{\varphi_f}$ approaches the model for nearfield case in (1). This can be explained by two logics: Firstly, the core property of this model is the separation of IRS depended and independent channel coefficients, which fits the fact of IRS nearfield application. Secondly, although the illumination path is merged into the IRS coding pattern for nearfield application, it can be also considered as an individual term which approaches the farfield channel model. Both of the clues above support that (4) might be suitable for both application types.

Afterwards, assume transmitting K times Tx symbols in separate steps as pilot for channel estimation, the received signal becomes a vector as

$$\boldsymbol{s_{Rx}} = \boldsymbol{h}\boldsymbol{S_{Tx}} + \boldsymbol{w}. \tag{5}$$

The transmit symbols are located at the diagonal elements of $\boldsymbol{S}_{Tx}$, and h is extended to $\boldsymbol{h} = \boldsymbol{h_f}\boldsymbol{\Phi_f}$, with $\boldsymbol{\Phi_f} = [\boldsymbol{\varphi_1}, ..., \boldsymbol{\varphi_K}]$. By operating a LS method, the estimated equivalent channel becomes

$$\hat{\boldsymbol{h}} = \boldsymbol{s}_{Rx}\boldsymbol{S}_{Tx}^{-1} + \boldsymbol{w}\boldsymbol{S}_{Tx}^{-1}. \tag{6}$$

If the IRS phase shift matrix $\boldsymbol{\Phi_f}$ is designed with full rank, the estimated wireless channel is

$$\hat{\boldsymbol{h}}_{\boldsymbol{f}} = \hat{\boldsymbol{h}}\hat{\boldsymbol{\Phi}}_{\boldsymbol{f}}^{-1} = \boldsymbol{h_f} + \boldsymbol{h_m}. \tag{7}$$

The vector $\boldsymbol{h_m}$ is the channel estimation error, with the mean square error (MSE) following [13] computed to be proportional with the trace of the matrix $(\boldsymbol{\Phi_f}^H \boldsymbol{\Phi_f})^{-1}$. To minimize the MSE, the Hadamard matrix is suggested for its perfect orthogonality. However, to achieve a proper channel estimation, the dimension of $\boldsymbol{\Phi_f}$ has to be $K = MN + 1$ to achieve the CSI derivation of the MN IRS units and the 1 constant contribution h_c. This number is not always satisfying the orthogonal dimension l for the Hadamard criterion. As a solution, a truncated Hadamard matrix from [13] takes the minimum l following $l > K$ and utilizes only the first K rows and columns of the Hadamard matrix with dimension l to formulate $\boldsymbol{\Phi_f}$. With this algorithm, the difficulties of IRS channel estimation mentioned in [7] have chances to be solved. Since a Hadamard matrix is formulated with -1 and 1 elements, this also fits the situation that the IRS demonstrations are mostly 1-bit phase resolution.

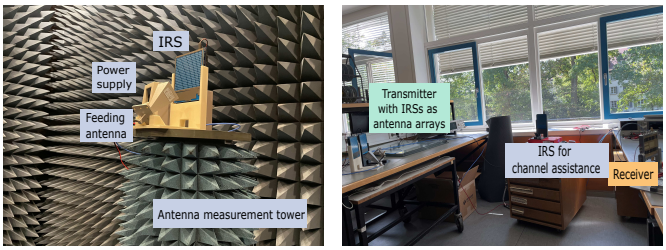

(a) IRS nearfield application setup. (b) IRS farfield application setup.

Fig. 2. Experimental IRS application types.

IV. IRS Testbed

The IRS utilized in this paper is the product from [2]. This is a 1-bit PIN-diode-based IRS with $M = N = 20$ units operating at 28 GHz. The setup for IRS nearfield application is presented in Fig. 2a, which behaves as an alternative antenna array. A holder ensures the optimized position of the feeding antenna for the maximized gain. For farfield application in Fig. 2b, the feeding antenna is further away from the IRS, and IRS behaves as a signal reflector with beamforming ability. The link distance in this setup is around 2 m.

The general testbed model keeps the similar architecture in [7] for further interest. For the proposed SISO scenario, a single feeding antenna, IRS, and receive antenna are implemented. For the signal propagation chain, software-defined radios (SDR) are the core components for the signal processing at the transmitter and receiver. To achieve the 28 GHz radio frequency (RF), RF frontend and backend modules are equipped. For the IRS control chain, the general idea is to pre-store required coding patterns in field programmable gate arrays (FPGAs), which control the voltages of the PIN-diode-based IRS units. After these coding patterns are examined, signal processing determines the optimum pattern and finalizes the IRS beamforming by sending a command to the FPGA via the Serial Peripheral Interface (SPI) bus. For the beam training algorithm, the pre-stored coding patterns correspond to beamforming patterns in different directions. The optimum DoD is determined among one of these beamforming directions based on the receiver power profile. For CSI-based channel estimation, the $K = MN + 1 = 401$ coding patterns following the truncated Hadamard matrix mentioned in Section III-B is pre-stored. The optimum pattern is then computed based on (7).

V. Result Analysis

In this section, the measurement results using the aforementioned channel estimation algorithms for different IRS application types are presented and compared. In general, signal propagation using 1 MHz bandwidth centralized at 28 GHz is occupied, and QPSK symbols are transmitted.

A. IRS Beam Training Results

Although beam training works for both IRS applications, the results for the nearfield case are neglected since they were intensively studied in [5], [7]. The measurement results for the IRS farfield application are presented in Fig. 3. For simplicity, the beam training covers $\theta = [0°, 2°, ..., 30°]$ with a constant ϕ. Three measurement results with the receiver located at

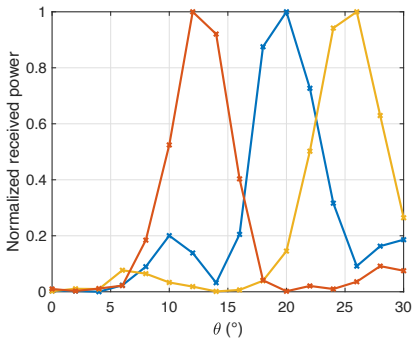

Fig. 3. Beam training results for IRS farfield application.

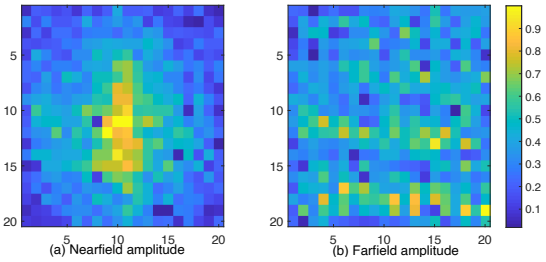

Fig. 4. Amplitude of CSI estimation for IRS units. The x and y axes denote the IRS unit indexes.

different positions with an illumination distance around 2 m are presented, showing good power behaviours with the optimum DoD observed. The results offer strong and novel evidence that the proposed beam training algorithm based on pre-designed beamforming patterns following (3) work properly.

B. IRS CSI Estimation Results

According to the equivalent channel model mentioned in (4), its form is approaching the nearfield model in (1). Therefore, the unit CSI estimation algorithm is expected to work also for nearfield application cases. Firstly, the measurement results for the amplitude of the IRS channel contribution from $\hat{\boldsymbol{h}}_{\boldsymbol{f}}$ in 7 are presented in Fig. 4. The results for nearfield application and farfield application are plotted in subfigures a and b, which are normalized separately to avoid undesired and focus only on the channel magnitude effects. For nearfield illumination, it can be observed that the high power is concentrated in the bottom middle position of the IRS. This point source illumination behavior fits the geometrical setup in Fig.2a perfectly. For farfield illumination, the amplitudes are more uniformly distributed through the units, obeying the plane wave behavior. The units with high/low amplitude levels in Fig. 4b are caused by the noise in the channel. This property is less obvious in nearfield case since it is masked by the strongly illuminated area. Nevertheless, this is only a visual property that does not influence the channel estimation results.

The phase distribution of CSI estimation is presented in Fig.5 for nearfield application. The phases are limited in the $-\pi$ to π range as the reference. Due to the geometrical placement, the estimated phase behaves as waves going upward as Fig.5a. Based on the phase of the estimated channel, the coding pattern of the implemented IRS can be determined with 1-bit quantization given by Fig.5b. The pattern has now

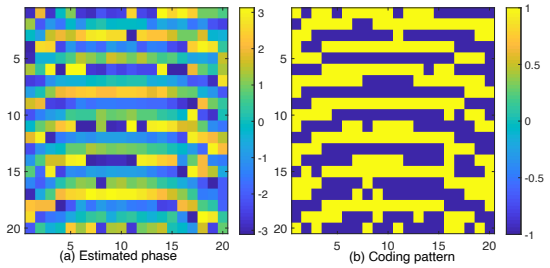

Fig. 5. Phase of IRS units for nearfield application. The x and y axes denote the IRS unit indexes.

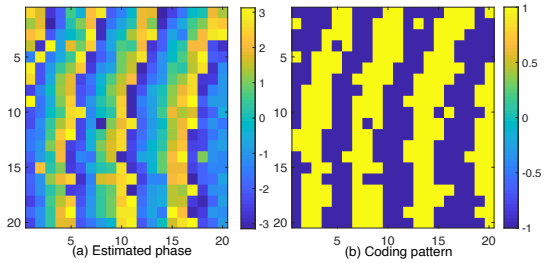

Fig. 6. Phase of IRS units for farfield application. The x and y axes denote the IRS unit indexes.

only -1 and 1 values denoting the on and off states of the PIN-diode-based IRS units. In this example, the receiver is located at 0° of the IRS, which leads to a very similar coding pattern as presented in [2]. The corresponding results for the farfield application are presented in Fig. 6. In this measurement, the feeding and receive antennas are located on the approximately same horizontal plane as IRS with a tilting angle as Fig. 2b. Therefore, the phase behaves as waves going left on the same plane. Same as before, with 1-bit quantization, the final coding pattern to formulate the communication path is determined.

C. Receive Power Observation

The accuracy of CSI estimation was proved by analyzing the geometrical logic regarding the patterns in the last section. However, the main idea for IRS coding pattern design is to derive an increased receive power to sufficiently prove the feasibility of the algorithms. Fig. 7 shows the receiver power performance for different application types and channel estimation algorithms over 10 measurements. In general, the CSI-based pattern in blue color outperforms the pre-designed beam training pattern in red color. The farfield application type benefits more due to the stronger possible LoS path in the h_c contribution of (4).

D. Path Analysis

As an important parameter, it is necessary to check the contribution of the estimated h_c from the total channel contribution h in (4), after the coding pattern is determined based on the IRS unit CSI. Fig.8a shows the comparison of channel contributions for IRS nearfield application, by taking the first three measurements from Fig.7a. It can be observed that the h_c contribution is very small, due to the fact that the feeding antenna is totally looking to the IRS as in Figure 2a. In this case, the h_c is only caused by some minor reflections

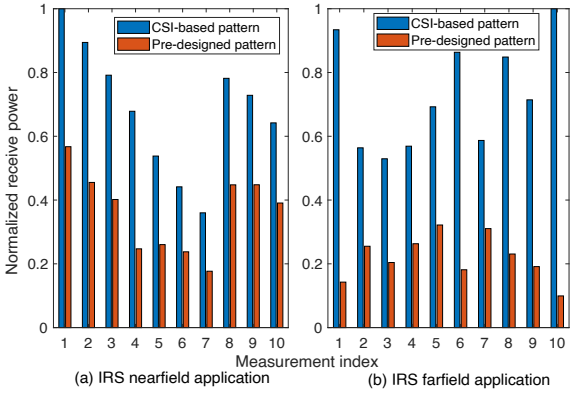

Fig. 7. Normalized receive power for different application types and channel estimation algorithms.

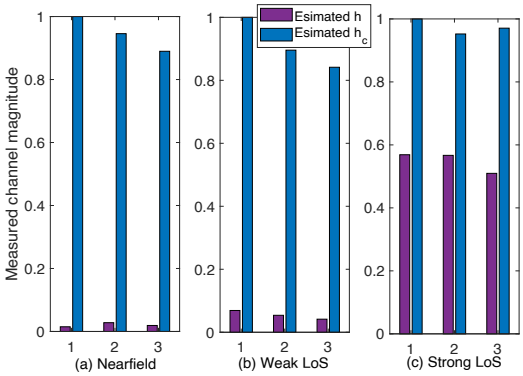

Fig. 8. Normalized channel magnitude for different channel contributions in different IRS measurement scenarios.

introduced by the indoor environment. For Fig.8b, the IRS farfield application taking the first three measurements from Fig.7b raises the contribution of h_c due to the possible LoS path between transmitter and receiver. However, its value is still very small because the feeding antenna is mainly looking at the IRS, and the LoS path is only occupied by the sidelobes. For comparison, Fig.8c shows measurements when the transmit antenna looks more into the receiver direction, and a significant increase of h_c is observed. These measurements prove the accuracy of the proposed channel estimation algorithm.

Comparing Fig.7 and 8, it can be observed that although the h_c part is small, the improvement of receive power is relatively large for the coding patterns finalized based on the IRS unit CSI. This is because the IRS unit CSI channel estimation has two more benefits besides the consideration of h_c contribution: Firstly, due to the pre-designed coding pattern for beam training, there is always a beamforming angle resolution to prevent infinite time consumption, which is 2° in this paper. Therefore, when the exact DoD is between the 2° increment, beam training only offers us a sub-optimum solution. Secondly, in practice, it is not always possible to promise that the receiver is located exactly in the planes for beam training, especially when the results in Fig.7 define a constant ϕ. The aforementioned mismatches are solved by the unit cell CSI estimation since this algorithm provides us channel coefficients instead of angle-dependent information.

VI. Conclusion

In this paper, IRS nearfield and farfield application types are for the first time compared with different channel estimation algorithms experimentally. The beam training algorithm is adapted to the IRS farfield application with proper accuracy. The theoretical channel estimation algorithm based on CSI estimation at each IRS unit is novel adapted to the IRS testbed. Its accuracy is proved in both IRS application types with improved performance in comparison to the conventional beam training algorithm. This paper is an important milestone for the theoretical IRS studies in the past years approaching practical utilizations.

Acknowledgment

This work was supported by the Federal Ministry of Education and Research of Germany in frame of the Open6GHub project under grant number 16KISK010.

References

[1] T. J. Cui *et al.*, "Coding metamaterials, digital metamaterials and programmable metamaterials," *Light: Science & Applications*, vol. 3, no. 10, p. e218, 2014.

[2] X. Wan *et al.*, "Reconfigurable sum and difference beams based on a binary programmable metasurface," *IEEE Antennas and Wireless Propagation Letters*, vol. 20, no. 3, pp. 381–385, 2021.

[3] W. Tang *et al.*, "Wireless communications with reconfigurable intelligent surface: Path loss modeling and experimental measurement," *IEEE Transactions on Wireless Communications*, vol. 20, no. 1, pp. 421–439, 2020.

[4] X. Wan *et al.*, "Multichannel direct transmissions of near-field information," *Light: Science & Applications*, vol. 8, no. 1, pp. 1–8, 2019.

[5] Y. Li *et al.*, "A programmable metasurface based tdma fast beam switching communication system at 28 ghz," *IEEE Antennas and Wireless Propagation Letters*, 2021.

[6] ——, "Beamsteering for 5g mobile communication using programmable metasurface," *IEEE Wireless Communications Letters*, 2021.

[7] ——, "Programmable metasurface hybrid mimo beamforming: Channel estimation, data transmission, and system implementations at 28 ghz," *IEEE Systems Journal*, 2022.

[8] C. Huang *et al.*, "Reconfigurable intelligent surfaces for energy efficiency in wireless communication," *IEEE Transactions on Wireless Communications*, vol. 18, no. 8, pp. 4157–4170, 2019.

[9] Q.-U.-A. Nadeem *et al.*, "Intelligent reflecting surface assisted wireless communication: Modeling and channel estimation," *arXiv preprint arXiv:1906.02360*, 2019.

[10] J. Chen *et al.*, "Channel estimation for reconfigurable intelligent surface aided multi-user mimo systems," *arXiv preprint arXiv:1912.03619*, 2019.

[11] B. Ning *et al.*, "Channel estimation and transmission for intelligent reflecting surface assisted thz communications," in *ICC 2020-2020 IEEE International Conference on Communications (ICC)*. IEEE, 2020, pp. 1–7.

[12] X. Pei *et al.*, "Ris-aided wireless communications: Prototyping, adaptive beamforming, and indoor/outdoor field trials," *IEEE Transactions on Communications*, vol. 69, no. 12, pp. 8627–8640, 2021.

[13] C. You, B. Zheng, and R. Zhang, "Intelligent reflecting surface with discrete phase shifts: Channel estimation and passive beamforming," in *ICC 2020-2020 IEEE International Conference on Communications (ICC)*. IEEE, 2020, pp. 1–6.

[14] A. Yu *et al.*, "Aperture efficiency analysis of reflectarray antennas," *Microwave and Optical Technology Letters*, vol. 52, no. 2, pp. 364–372, 2010.

[15] A. Alkhateeb *et al.*, "Channel estimation and hybrid precoding for millimeter wave cellular systems," *IEEE Journal of Selected Topics in Signal Processing*, vol. 8, no. 5, pp. 831–846, 2014.